

## Article

# High-Resolution Mapping of Seasonal Crop Pattern Using Sentinel Imagery in Mountainous Region of Nepal: A Semi-Automatic Approach

Bhogendra Mishra <sup>1,2,3,\*</sup> , Rupesh Bhandari <sup>1,4</sup>, Krishna Prasad Bhandari <sup>1</sup>, Dinesh Mani Bhandari <sup>1</sup> ,  
Nirajan Luintel <sup>3</sup>, Ashok Dahal <sup>5</sup> and Shobha Poudel <sup>2,3</sup> 

<sup>1</sup> Center for Space Science and Geomatics Studies, Institute of Engineering, Pashchimanchal Campus, Tribhuvan University, Pokhara, Nepal

<sup>2</sup> Policy Research Institute, Narayanhiti, Kathmandu, Nepal

<sup>3</sup> Science Hub, Kathmandu, Nepal

<sup>4</sup> Department of Geography, University of Alabama, Tuscaloosa, AL 35487, USA

<sup>5</sup> ITC, the University of Twente, 7522 Enschede, The Netherlands

\* Correspondence: bmishra@sciencehub.org.np

**Abstract:** Sustainable agricultural management requires knowledge of where and when crops are grown, what they are, and for how long. However, such information is not yet available in Nepal. Remote sensing coupled with farmers' knowledge offers a solution to fill this gap. In this study, we created a high-resolution (10 m) seasonal crop map and cropping pattern in a mountainous area of Nepal through a semi-automatic workflow using Sentinel-2 A/B time-series images coupled with farmer knowledge. We identified agricultural areas through iterative self-organizing data clustering of Sentinel imagery and topographic information using a digital elevation model automatically. This agricultural area was analyzed to develop crop calendars and to track seasonal crop dynamics using rule-based methods. Finally, we computed a pixel-level crop-intensity map. In the end our results were compared to ground-truth data collected in the field and published crop calendars, with an overall accuracy of 88% and kappa coefficient of 0.83. We found variations in crop intensity and seasonal crop extension across the study area, with higher intensity in plain areas with irrigation facilities and longer fallow cycles in dry and hilly regions. The semi-automatic workflow was successfully implemented in the heterogeneous topography and is applicable to the diverse topography of the entire country, providing crucial information for mapping and monitoring crops that is very useful for the formulation of strategic agricultural plans and food security in Nepal.

**Keywords:** Sentinel 2; crop pattern; crop calendar; NDVI; Nepal



**Citation:** Mishra, B.; Bhandari, R.; Bhandari, K.P.; Bhandari, D.M.; Luintel, N.; Dahal, A.; Poudel, S. High-Resolution Mapping of Seasonal Crop Pattern Using Sentinel Imagery in Mountainous Region of Nepal: A Semi-Automatic Approach. *Geomatics* **2023**, *3*, 312–327. <https://doi.org/10.3390/geomatics3020017>

Academic Editor: Abdul M. Mouazen

Received: 22 February 2023

Revised: 22 March 2023

Accepted: 4 April 2023

Published: 6 April 2023



**Copyright:** © 2023 by the authors. Licensee MDPI, Basel, Switzerland. This article is an open access article distributed under the terms and conditions of the Creative Commons Attribution (CC BY) license (<https://creativecommons.org/licenses/by/4.0/>).

## 1. Introduction

The demand for food is expected to increase from 59% to 98% by 2050 (Valin et al., 2014) due to the increasing population and economic growth that increase per capita consumption [1]. In order to supply the increasing demand for food, crop production will need to be increased by either increasing the area of agricultural land or enhancing productivity. Several other factors, such as increasing climatic variability, urbanization, and lack of investment, etc., will make it challenging to produce enough food [2]. The ecological and social trade-offs of converting more land to agriculture are full of dispute and are not possible in many places. The only possible option would be to intensify the cultivation and enhance the productivity of existing agricultural land through modern varieties of crops and better crop management.

Considering the increasing climatic variability and changes in technological and socioeconomic factors, the introduction of modern varieties of crops and better farm management are the available options for increasing productivity [3]. Besides, climatic and

socioeconomic factors cause the inter-annual fluctuation of planting and corresponding harvesting dates, adding to the challenges of optimal farm management. Tracking such variations in crop dynamics in a heterogeneous topography, such as Nepal, is challenging due to the complexity of the multi-crop environment, fragmented plot sizes, changes in technology, farm management practices, and climatic conditions [4–6].

Optimal management of crops requires detailed information on when and where a particular crop is being planted. Updated information on the cultivation area and their seasonal dynamics helps to address such ever-growing issues that can facilitate a better crop management plan such as timely crop seed supply, fertilizer supply, training, and capacity building of farmers to improve productivity, etc. This is important for proper storage planning and supply chain management, which could contribute to policy development for decision-makers.

Knowledge of where and when crops are grown provides insights into the ecology and ecosystem balance of the region. The extent of agricultural land, cropping intensity, and phenology of the crops affect the interaction in the ecosystem and its services at the local as well as regional levels. Information on these aspects can act as a decision support tool for a stakeholder to reach sustainable land-use management. Since agriculture uses resources such as water, nutrients, and carbon, as well as the biodiversity in the region in the process of growth and production, it creates a strong chain in the transfer of material and energy in the ecosystem [7]. Agriculture as a component of the ecosystem affects and is affected by the environment, it therefore has multiple interactions in the ecosystem viz. pollination, pests, soil symbiosis, and the carbon cycle, among others [8–11].

In addition to an areal extent, the timing and cropping intensities of crops are important determinants of the ecosystem. For instance, the increased cropping intensity of the same crop has been linked to reduced ecosystem services such as pollination and pest control due to an overuse of resources, thereby threatening the sustainability of the agriculture yield [12]. Moreover, the phenology of the crops influences the plant-pollinator interaction whereby the overall state of the ecosystem, as well as the productivity of the crop, is determined [13]. For example, the larger overlap period between the crops growing stage and insect larval stage puts crops under greater threat, while that between the crop flowering stage and insect matured stage increases pollination and hence production [8,9]. Hence, the mapping of crops and crop phenology is an important aspect of the ecology.

Phenological analysis of crops through time-series remote sensing images allows the monitoring of the seasonal dynamics of crops that can capture significant agricultural activity, i.e., sowing, transplanting, and harvesting dates of an area [5]. The increasing availability of spatial and temporal resolution satellite images allows us to monitor crop phenology at regular intervals. The uses of the remote sensing-based vegetation index (VI) have already been widely accepted to monitor crop growth at a global, regional and field scales [14–17]. Furthermore, a number of studies in the past have acquired the precise phenological stages such as the start of the season (SOS), the peak of the season (PoS), or end of the season (EoS) at the pixel level from the phenological curve derived from remote sensing images [18–20]. The cropping intensity of a region can be derived once the key phenological stages are identified. In addition, the detection of uncultivated arable land in a particular season provides an opportunity to intensify the cropping pattern and increase production.

Mapping of cropping intensity using low to moderate spatial resolution [21] (i.e., NOVA-AVHRR, MODIS) remains a challenge in Nepal due to a large number of smallholder farmers [22] and very complex terrain. The size of plots are usually smaller than a single pixel [0.7 ha of average farm size [23] vs. 6.25 ha of MODIS image, approximately 100 ha for AVHRR] and multiple cropping patterns which results in subpixel heterogeneity in crop intensity and type identification. An alternative higher resolution images such as Sentinel dataset with 10 m spatial resolution can be used to overcome this subpixel heterogeneity problem by applying the temporal mixture analysis for fragmented farms [16]. However, this dataset has not been fully explored to keep track of the phenological stages (i.e., crop calendar in the mountainous topography) of a country like Nepal. On the other hand, a high-resolution crop cycle inventory and precise crop areas are not yet available [24] although they are essential for better crop planning and management and for improving agricultural production. Therefore, knowledge about the seasonal extension of cropping patterns in Nepal remains limited and accurate cropping intensity maps are in urgent need. This study aims to fill this gap by using remote sensing-based data along with farmer knowledge at the field level.

The objectives of this study are: (i) to develop a semi-automatic workflow to develop a high-resolution crop calendar, (ii) to integrate the crop calendar and farmer knowledge to produce the cropping maps, and (iii) to assess the spatiotemporal dynamics of cropping intensity in Kaski, Nepal. The results will be important when developing agricultural policies for decision-makers. The knowledge of precise harvesting dates are useful in relation to food security, for planning and developing mobilization of food aid, and proper storage planning, all of which could contribute to the united nations (UN) sustainable development goal (SDG#12.3) [4].

## 2. Study Area

Kaski district extends from the mid-hilly region to the High Mountainous region of Nepal and is geographically between 28.09 °N to 28.42 °N latitude and 83.68 °E to 84.14 °E longitude Gandaki Province, with a total area of 2017 km<sup>2</sup>. Figure 1 depicts the land cover map of Kaski district. The elevation of the Kaski district ranges from the lowest land of 450 to 8091 m (Mt. Annapurna I). The climate varies based on altitude, from subtropical in the lowest altitude region of the district to temperate and subalpine to alpine. The low altitude subtropical areas are warm for most of the year, while the mountains in the north have a temperate climate [25]. The district receives approximately 2710 mm of precipitation annually. Approximately 70% of the annual precipitation occurs during the rainy season from June to September [26]. The total agricultural area of Kaski district is 19,200 ha [27]. In summer, the principal crop types are rice and millet planted from June to August and harvested from September to November; maize is a spring crop planted from March to April and harvested from June to July; and wheat, potato, and buckwheat are winter crops planted from November to January. Winter vegetables are also common in the district, but are often planted in a minimal plot smaller than one ropani (504 m<sup>2</sup>), the most commonly used local unit of land, and are usually grown for domestic uses. Forest and snow cover dominate land cover types in the higher altitude areas, while in the south, it is cultivated.

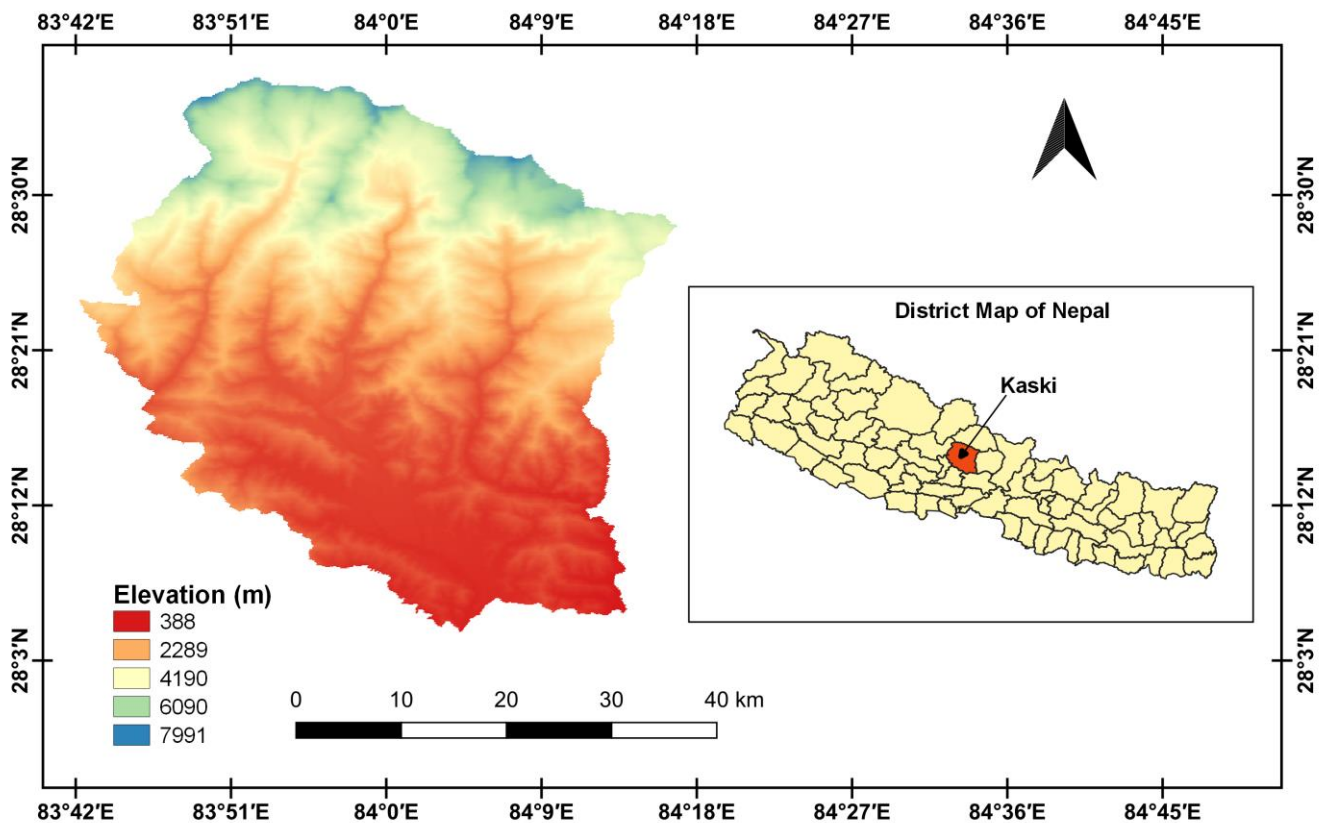


**Figure 1.** This map shows the study area, Kaski district, Nepal, along with the land cover classification. The land cover data was sourced from ICIMOD (International Centre for Integrated Mountain Development).

### 3. Data and Method

We refined, extended, and automated the remote sensing-based methods to keep track of the season's crop dynamics and computation of crop intensity through phenology based on Sentinel 2 A/B images of the high mountainous areas to the hill with a plain valley, to develop a high-resolution crop calendar. We first delineated the agricultural area through unsupervised ISOData clustering within the topographically cultivable area and employed a rule-based algorithm on time series Sentinel 2 normalized difference vegetation index (NDVI). The overall process flow is depicted in Figure 2, and the details of each step are elaborated in the subsequent subsections.

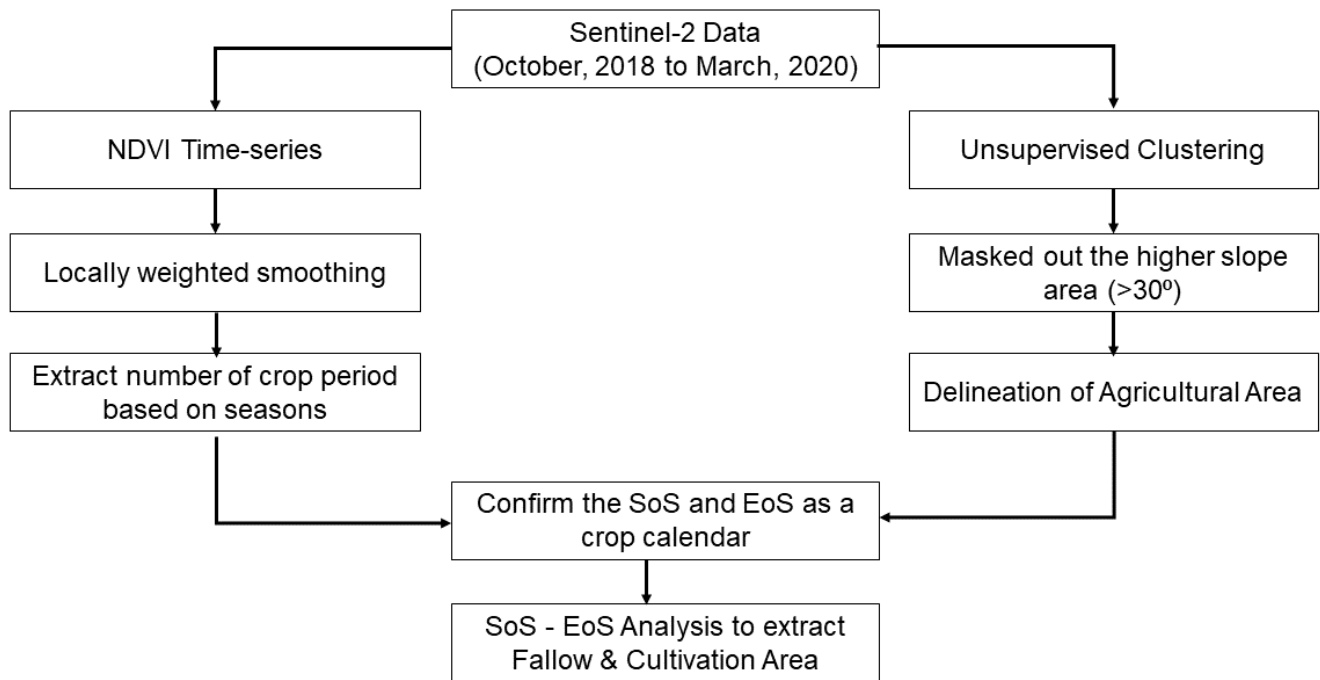


**Figure 2.** This diagram illustrates the overall research design used to estimate agricultural areas and extract seasonal dynamics using remote sensing techniques.

### 3.1. Remotely Sensed Dataset

The present study used Sentinel 2 A/B images available every five days at a 10 m spatial resolution in the visible and near-infrared bands. The images from October 2018 and February 2020 were used for the time-series analysis. We obtained the Surface Reflectance (Bottom of Atmosphere) data of product level 2A from the Google Earth Engine (GEE). The product was already orthorectified and performed atmospheric correction. A Global Digital Elevation Model (GDEM) from the Advanced Spaceborne Thermal Emission and Reflection Radiometer (ASTER) with a spatial resolution of 30 m was also acquired.

### 3.2. Field Based Data

Field plot data were collected between April and May 2019. Questionnaire surveys with farmers and agricultural extension officers were conducted to determine cropping types and calendars across the district. This information includes a list of common crops planted in different seasons, crop calendars, and cropping intensity (single, double, or triple crop). In order to access the mapping accuracy, a total of 385 locations, as shown in Figure 3, were selected as ground truth points, based on the knowledge of local agricultural extension officers, to ensure that the sample size was adequate, out of which we visited 240 locations. This covered the major crop-land areas and other landcover types. For the remaining 145 locations, primarily located in high-altitude areas, we used high-resolution Google Earth images. Garmin GPSMap 64 and Garmin eTrex30 series handheld devices were used to record the geographical coordinates. All points (385), which included agricultural and nonagricultural classes, were used for the accuracy assessment. At each of the field locations, the following data were recorded for 2019.

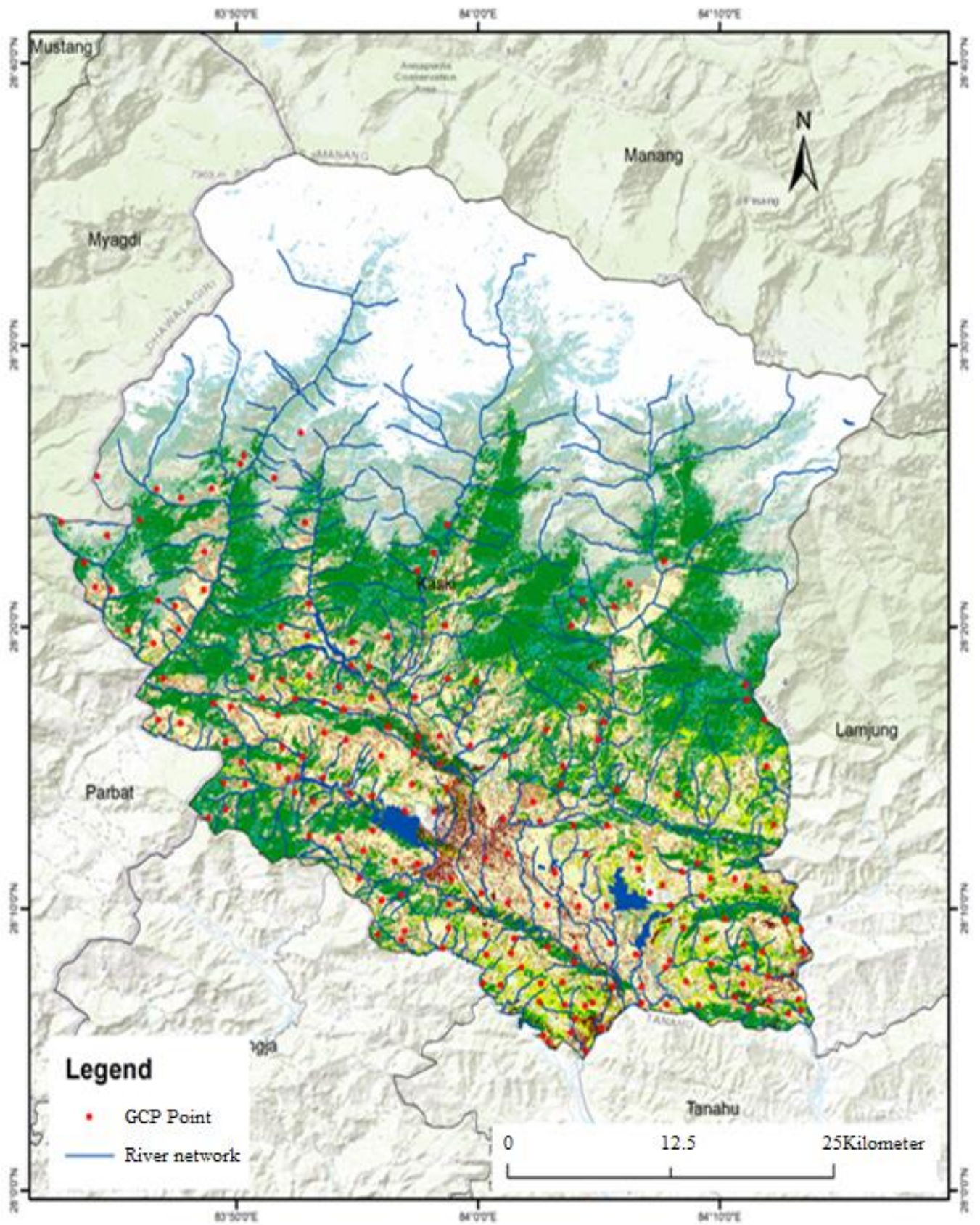


**Figure 3.** Location of the ground-truthing sites, the red dots on top of a land cover map of Kaski district overlaid on the OSM terrain.

- i. Land-use parameters such as cropland, rangelands, forest, etc.
- ii. Cropping calendars for monsoon, winter, and autumn seasons for an agricultural area
- iii. Irrigation (also seasonal) availability.

The NDVI values were computed by combining timeseries NDVI values into a single-file data cube subjected for the agricultural area delineation and phenological analysis. The NDVI is the normalized difference ratio between the reflectance measured at the red and near-infrared (NIR) bands (Equation (1)).

$$NDVI = \frac{NIR(842 \text{ nm}) - Red(665 \text{ nm})}{NIR(842 \text{ nm}) + Red(665 \text{ nm})} \quad (1)$$

The unsupervised clustering Iterative Self-Organizing Data Analysis (ISODATA) technique [28] was applied to the NDVI time-series of eight images (cloud-free) around the year to generate the initial classes. A maximum of 50 iterations and a convergence threshold of 0.99 were set for the clustering. The number of clusters varied from 5 to 10. NDVI temporal signatures and ground survey data were used to convert the clusters into land cover classes, such as agricultural, built-up, barren, forest, grass, snow, and water. The agricultural area was further used to determine the seasonal crop extent and crop calendar, which consists of the following major steps: (i) NDVI time-series generation, (ii) data filtering and smoothing, (iii) crop calendar estimation, and (iv) accuracy assessment.

### 3.3. Crop Calendar Estimation

The time-series NDVI dataset after the cloud mask was subjected to analysis. The missing dataset, (Figure 4a) due to the cloud contamination, was filled through the linear interpolation method to obtain the continuous-time series dataset, as shown in Figure 4b. To smooth the image time series of individual pixels, we applied a locally estimated scatterplot smoothing (LOESS) filter [29–31]. The filter was applied using linear regression with a moving window of size 11. The window size of 11 was set after multiple trials and errors. The outcomes of the multiple trials can be seen in Figure 4c.

The crop calendar, the classification of different physiological stages of a crop during its growth cycle [32], consists of crucial phenological information ranging from land preparation to harvesting dates. The start of the season (SoS) is referred to as the period before sowing. The end of the season (EoS) is referred to as the period after harvest. The smoothed time-series data identified the local maxima and minima, as shown in Figure 4c. This local minima, maxima, and minima duration is considered a valid crop cycle and an indicator of the number of cropping seasons detected. The following conditions have been set to detect the crops and their phenological stages (i) average annual NDVI value is below 0.25, which was found empirically with the known agricultural area, and (ii) a consistent NDVI increment after the detected minima, (iii) the maximum NDVI is above 0.4, and (iv) the range of days in between minima and maxima of the valid crop cycle was within 60 to 120 days. Finally, the number of cropping cycles was determined by counting the seasonal peaks in each year. The source code of every process is available in Supplementary Material.

### 3.4. Accuracy Assessment

The accuracy assessment was performed based on the field-based survey data points, as shown in Figure 3, and a confusion matrix was generated for the land cover and crop intensity, respectively. The overall accuracy, producer accuracy, user accuracy, and Kappa coefficient were computed to ensure the accuracy, which provides a measure of agreement between the model predictions and reality obtained from the field visit.

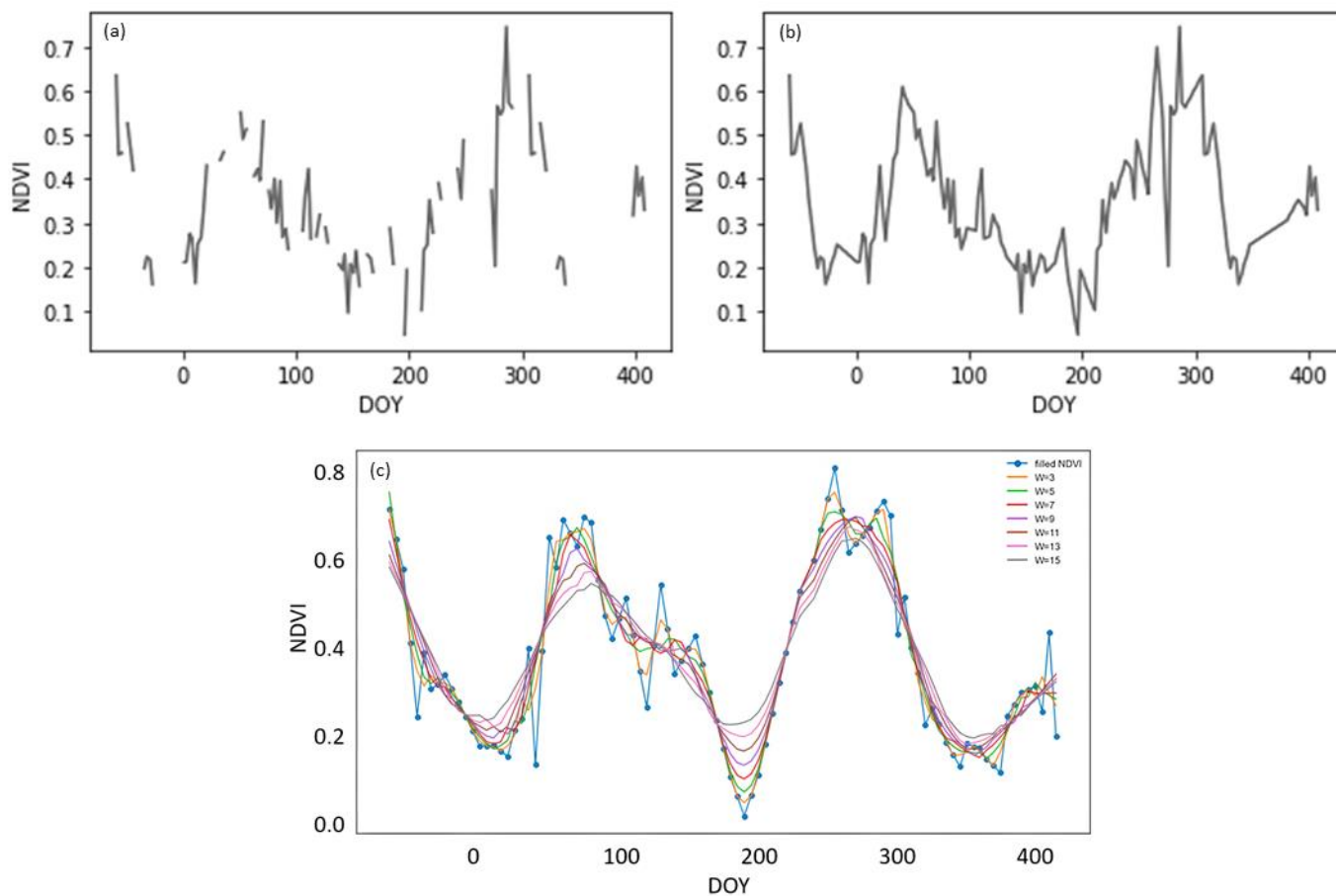


**Figure 4.** Temporal profile of NDVI value over a year after filtering out the cloud-contaminated pixels (a), after filling the gap through linear interpolation (b), and smoothing results that are subjected to analysis to find the crop calendar (c).

## 4. Results and Discussion

### 4.1. Agriculture Map

Figure 5a illustrates the land cover map for the Kaski district based on ISODATA clustering followed by post-processing classification, and Figure 5b shows the delineated agricultural areas. Table 1 shows the error matrix based on the ground observations. The overall accuracy was 81.34%, and the Kappa coefficient was 0.74. The user's accuracy in the agricultural area was 93.59%, whereas the producer's accuracy was 91.82%.

The arable land is concentrated in the southern and southeastern parts of the district along the Seti River Basin up to 3000 m, and sparse arable land is distributed in the higher elevation zone. A total of 21,404 ha of the area is identified as agricultural area, which is approximately 10% (2204 ha) higher than the agricultural area recorded by the Ministry of Agriculture (19,200 ha) [27]. The error of commission arises from forest and grassland being misclassified as an agricultural class, as the grassland has a very similar attribute to the single-season agricultural area, i.e., the grasses grow in monsoon and reach a peak in mid-September, which is very similar to the timing of rice and millet. Similarly, the riverbanks next to the paddy field were covered by grass during this season. Therefore, the agricultural area in one season is slightly overestimated. However, detecting the phenological cycle of non-cultivated vegetation in winter and spring is sporadic, and if any, the phenological cycle is not similar to that of any crops. There could be a rare chance to have a similar pattern to the crops in the winter season, but this is often very short in duration, and the



NDVI usually does not reach the minimum requirement of the maximum NDVI value, i.e., 0.4.

Most of the area in the north is a higher mountainous region with a perennial snow cover area (above 4000 m elevation) and a steep slope, so the arable land is less in proportion. Among the five local units, namely Annapurna, Machhapuchhre, Madi, Rupa and Pokhara, most of the agricultural land falls into the Pokhara Leknath metropolitan city, as shown in Figure 5b.

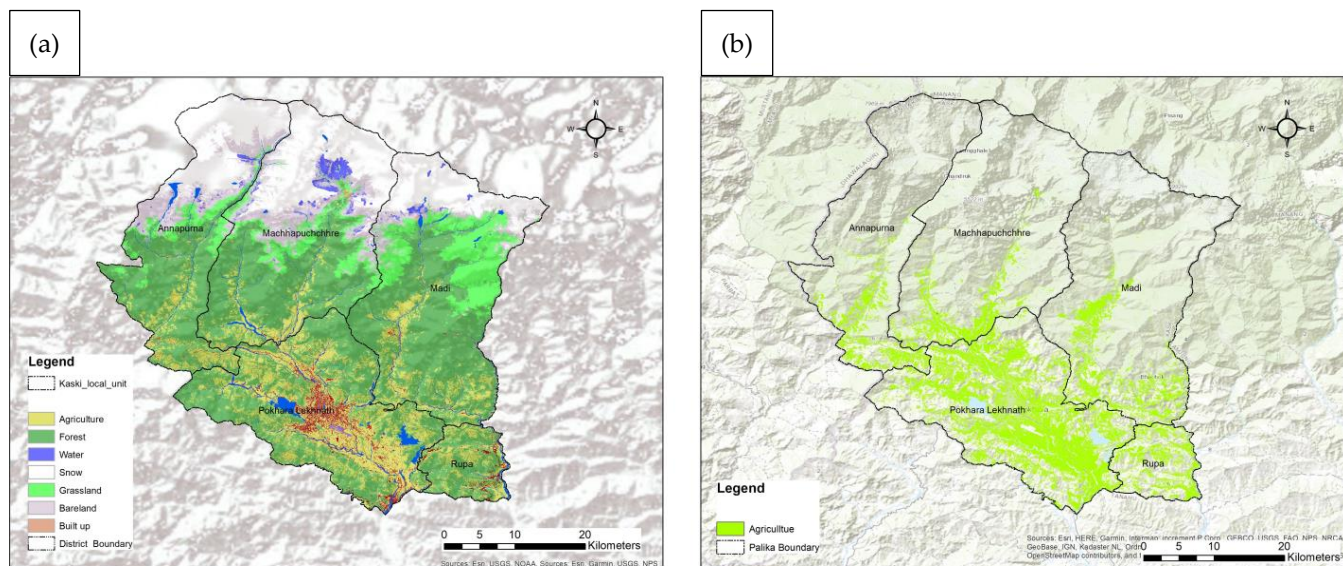


**Figure 5.** Agricultural area in Kaski, Land cover map—(a) and agricultural area only (b) over the topography background of ArcGIS.

**Table 1.** Error matrix obtained based on the ISODATA clustering followed by post-processing.

		Observed Data							Total	Users Accuracy
		Agriculture	Forest	Water	Snow	Grassland	Bareland	Built up		
Classified data	Agriculture	146	3	0	0	5	2	0	156	93.59
	Forest	6	27	0	0	9	0	0	42	64.29
	Water	2	0	12	0	0	0	0	14	85.71
	Snow	0	0	2	6	0	2	0	10	60.00
	Grassland	3	3	0	0	14	0	0	20	70.00
	Bareland	2	0	0	0	2	32	8	44	72.73
	Built up	0	0	0	0	4	11	42	57	73.68
	<b>Total</b>	159	33	14	6	34	47	50	343	
<b>Producers Accuracy</b>		91.82	81.82	85.71	100.00	41.18	68.09	84.00		81.34

#### 4.2. Crop Calendar

We identified a maximum of three crop cycles in a year through the time-series NDVI analysis between October 2018 to March 2020. The first season was February-April to June-September, the second crop season was May-August to September-December, and the third was November-December to February-May. The division of seasons is based on the field visit and the phenological changes in the ground vegetation, while their names season 1, season 2, and season 3 are given arbitrarily.

We mapped the annual crop intensity of the Kaski district at a 10 m spatial resolution for the year 2019. Figure 6 shows the map of cropping intensity, Table 2 depicts the performance of the detected crop intensity, and Table 3 depicts the total area covered by agricultural land based on a multi-cropping pattern (i.e., one, two, and three-season crops). The areas cultivated with crops in all three seasons are mainly detected around the Pokhara valley, as the valley’s topographic characteristics and availability of irrigation facilities make it favorable for three cycles of cropping. Land with crops in two seasons are dominant

in the Pokhara Valley, including rice and millet during summer, and buckwheat, wheat, potato, and other seasonal vegetables during winter; the third season crops include maize, rice, and other vegetables where irrigation is available.

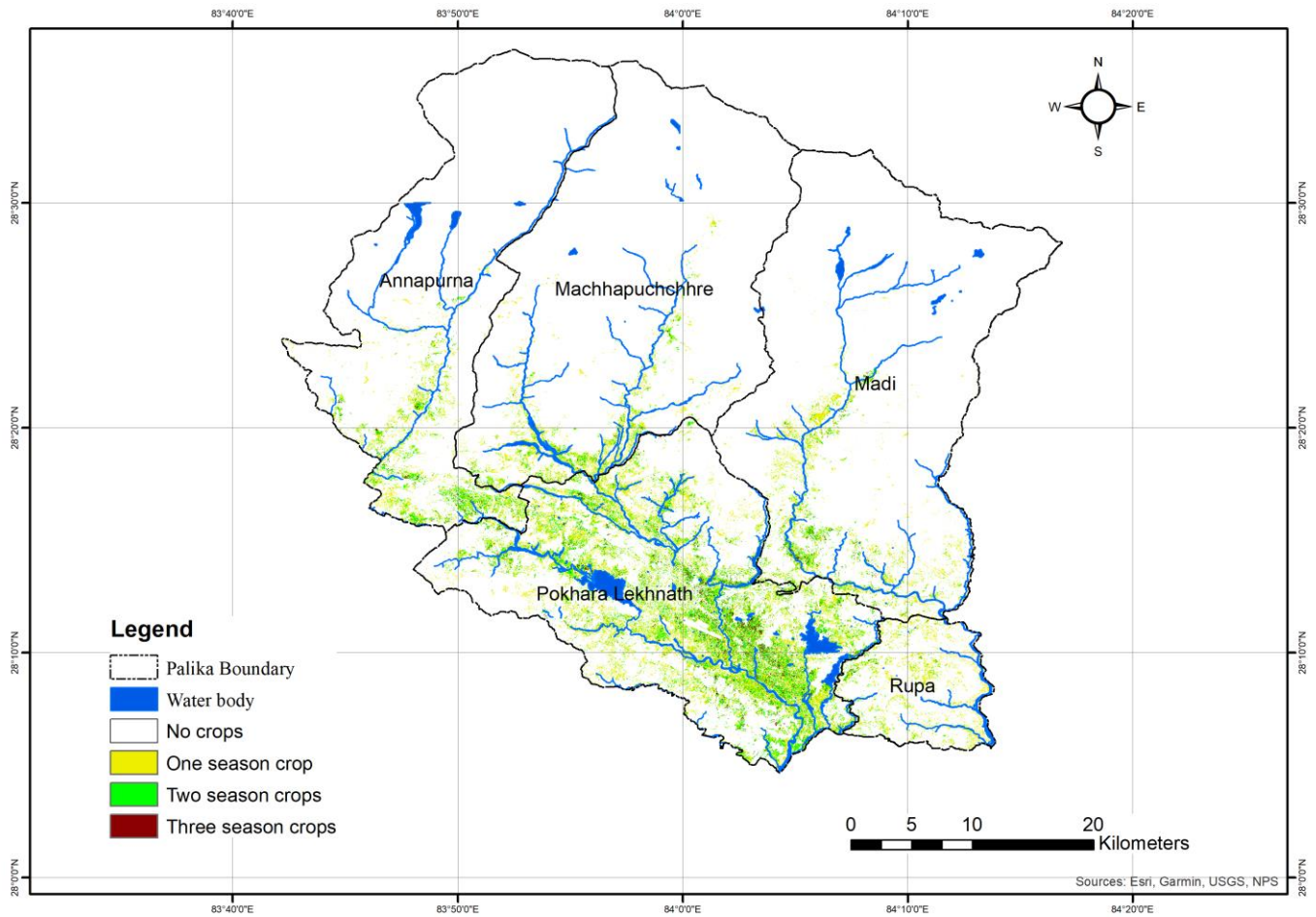


Figure 6. Crop intensity in Kaski District, shows the one, two, and three-season cropping areas.

Table 2. Error matrix of the crop intensity.

		Observation				Producers' Accuracy
		One	Two	Three	Total	
Classification	Intensity					
	One	66.00	6	0.00	72.00	91.67
	Two	2.00	44	4.00	50.00	88.00
	Three	0.00	3	21.00	24.00	87.50
Total		68.00	53	25.00	146.00	
Users accuracy		97.06	83	84.00		88.73

Table 3. Area of one season, two season, and three-season crops in Kaski in 2019.

Season	Area (ha)
One season	13,519
Two seasons	6721
Three seasons	1164

#### 4.3. Seasonal Crop Dynamics

Figure 7a,b illustrate the crop area and calendar of crops during season 1 in the Kaski district in 2019. The season starts in February–April and ends in June–September. The primary crop in season 1 is maize. Although there are spring rice plantations in some areas, and a few green vegetables were identified in this season, they were very fragmented and planted primarily for domestic purposes. Those planted for commercial purposes are usually in a greenhouse environment which is not visible in the satellite images. Therefore, we have not considered any other crops in this study. Maize is one of the major staple crops in Nepal and is equally popular from high-altitude areas to the southern plains. Maize is grown in almost all non-irrigated land (locally called *bari*) and paddy rice in all irrigated farmlands across the district during the summer, irrespective of location. More than 12,000 ha of spring crops were detected in the year 2019. This contributes to about 25% of the total crop area of the entire year. The local variants of maize are grown under rainfed conditions and mostly on marginal land with minimal chemical fertilizers; however, modern hybrid varieties were identified in the low valley area, where irrigation facilities are available and where the yield is better according to the farmers.

Similarly, the season 2 crop calendar in the Kaski district in 2019 is shown in Figure 7c at the start of the season and Figure 7d at the end of the season. The season starts in May–August and ends in September–December. The primary crop in season 2 is rice in the irrigated areas. At the same time, it is millet in a non-irrigated area, lentils are usually planted along with rice, especially in the edges of plots and near the river-sandy areas. Summer vegetables are also common, but they are very fragmented and planted for domestic purposes only. Rice transplantation typically started in mid-June and lasted until mid-August, whereas harvesting started from late September to early December. It is the summer crop that occupies the largest area of a single crop in this district. Most of the rice is transplanted in late June. The millet is transplanted from late May to late June, and harvested in November.

Figure 7e,f illustrate the crop dynamics in season 3 in the Kaski district in 2019 with the start of the season in Figure 7e and end of the season in Figure 7f. The season started in November–December and ended in February–May. During the winter season, varieties of vegetables, including potato, buck whites, spinach, cauliflower, broccoli, radish, caret, and various beans, etc., are cultivated across the district, and vegetables occupy the largest area among the crops in this season. Wheat and barley, along with other wheat families and buckwheat, are the other major crops grown in winter. Figure 7g illustrates the sampled area where one-, two-, and three-season crops were present. The majority of the area has a single rice crop from July to November. The figure shows the field preparation for rice transplantation in July, followed by the full flowering of rice in October, and the harvesting in November. After the rice harvest, the area remains fallow or is sown with potato or wheat in December, which becomes visible in January and is harvested in March. In April, a few areas have crops such as maize, while the majority remain fallow. As a result, some areas have only one crop, whereas others have two, and a few have all three crops.

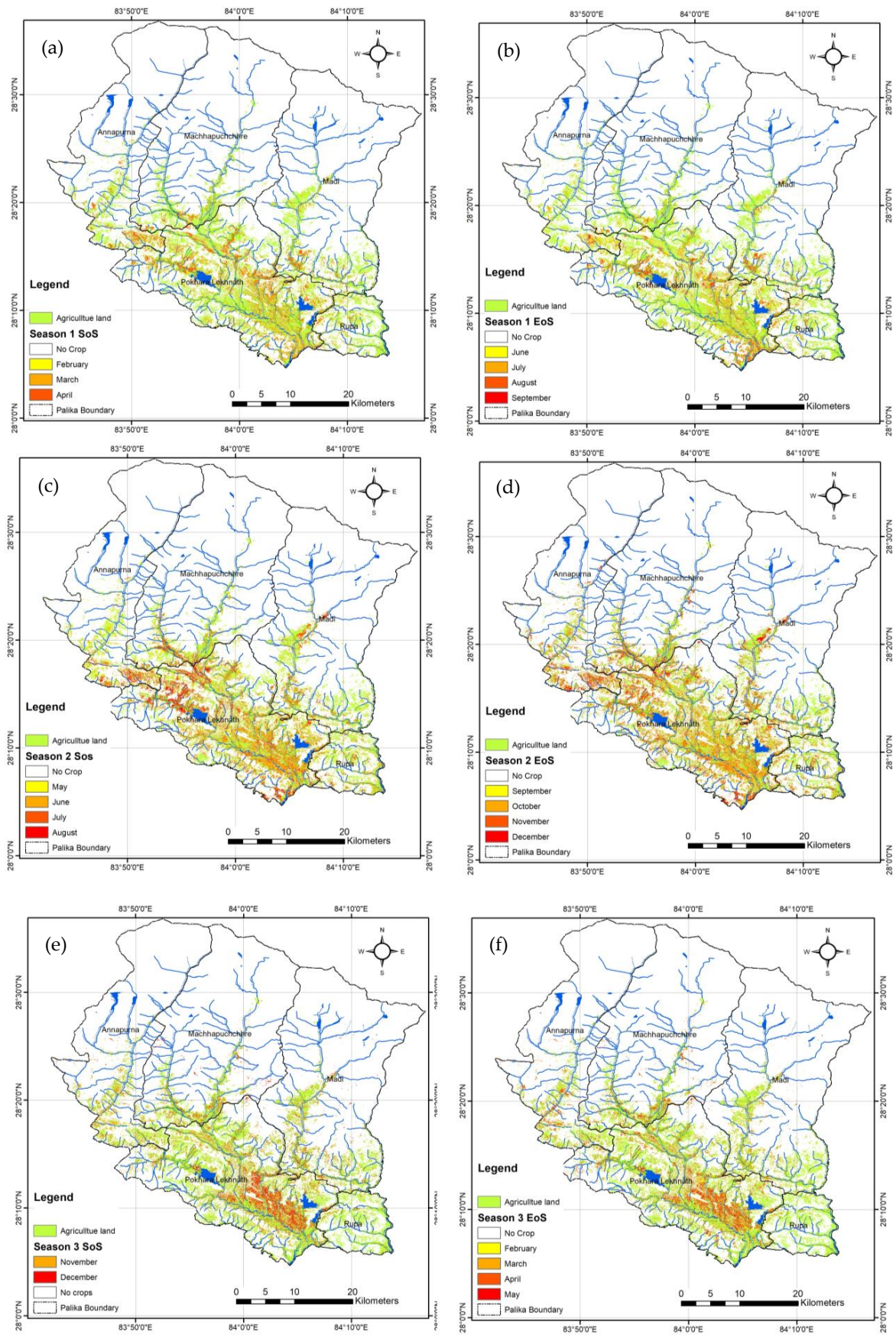
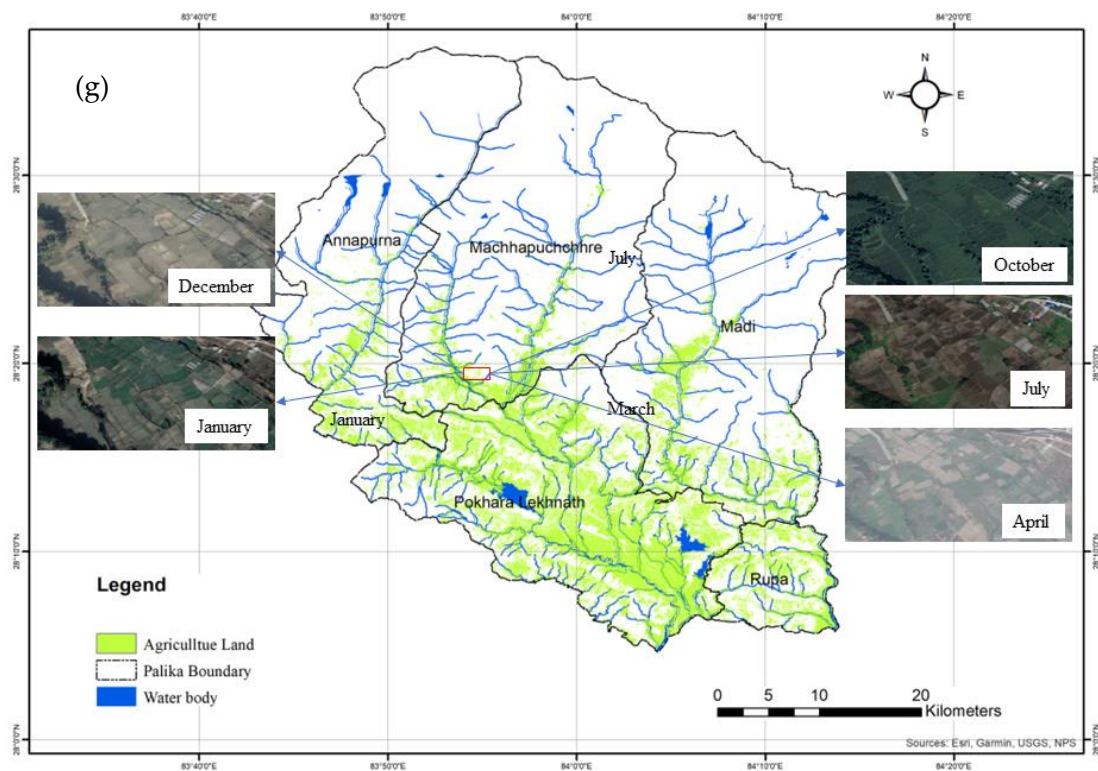


Figure 7. Cont.



**Figure 7.** The figure shows the timing of the agricultural cycle, where green represents the agricultural area. The Start of Season (SoS) and End of Season (EoS) are overlaid in yellow, orange, and red. The SoS and EoS are shown for the three seasons, with season 1 represented by panels (a,b), season 2 by panels (c,d), and season 3 by panels (e,f). Panel (g) shows the sampled area with a mix of one, two, and three-season crops.

#### 4.4. Discussion

In this study, agricultural land was delineated at high-resolution and seasonal dynamics of the crops, and eventually the cropping intensity, was computed using Sentinel 2-based NDVI time-series in the Kaski district of central Nepal through the automatic processing chain. This study established that the Sentinel-2 based dataset is useful for automatically tracking crop dynamics in small-scale farms with heterogeneous topography. Before this study, phenology estimation had been realized based on a field survey [33,34] or coarse resolution remote sensing data such as MODIS time-series data [24,35,36]. However, field observation is time and resource consuming; hence, it cannot be extended to a larger area. On the other hand, the use of coarse resolution remote sensing data does not provide reliable results for crop cycle mapping in hilly regions due to mixed pixel conditions.

Mapping and comparative analysis of cropping intensities over the years requires adequate quality and spatiotemporal accessibility of satellite datasets for key crop growth seasons. Sentinel 2 based method could accurately map the seasonal cropping patterns of smallholder farms where the size of one field (typically  $\leq 2$  ha) is smaller than the spatial resolution of readily available satellite data, like MODIS and Landsat. The coarse spatial resolution of the MODIS data limits its applicability for phenology extraction and crop mapping in heterogeneous landscapes with mixed pixels, such as those in the hilly regions of Nepal [36]. Further, crop mapping and phenology mapping using Landsat alone may not be sufficient due to its long (16-day) revisit time, as noted in reference [37]; in addition to that, a higher percentage of cloud cover (e.g.,  $>25\%$ ) limits the accessibility of good quality images during monsoon season in this region [38]. However, the Sentinel 2 images with a spatial resolution of 10 m [39] can detect small farms and frequently revisit (5-day) hence,

it is found to be highly useful for tracking the seasonal crop dynamics and eventually cropping intensity.

The extent of croplands and their seasonality are important aspects of the ecosystem, as crops are affected by the interactions in the ecosystem as well as the impact on the existing ecosystem. During the field visit, we confirmed that the dynamics of the seasonal cropping systems are dependent on various factors: the intrinsic characteristics of the ecosystem, including soil type, soil moisture, and soil nutrients, and on external factors such as elevation, rainfall, drought, availability of irrigation, especially in winter, and timely availability of fertilizers and seeds. The type of crop and its timing is affected by soil type and availability of soil moisture. Relatively higher winter rainfall and fertile alluvial soils offer sufficient soil moisture to raise winter and spring crops during the dry season, which begot a higher concentration of double or triple crop patterns in the Pokhara Valley. In contrast, higher elevation mountainous regions in the northern part where a dry and cold ecosystem prevails receive irregular and relatively less rainfall during dry seasons, which leads to inadequate soil moisture conditions to establish and grow any crop. Consequently, most cultivable land remains fallow during the dry season. Dryness could be a prominent factor that could affect the cropping intensity. The seasonal crop dynamics detected in this region supports these facts. The winter rainfall is irregular, and a dry winter spell reduces the winter cropping areas. Similarly, cropping in the summer season also depends on the timing and amount of rainfall.

Accurate and updated cropping intensity maps and their area statistics enables policy-makers to intensify cropping patterns and increase crop production primarily in single-crop areas. This study's comparative and temporal analysis of seasonal crop dynamics and intensity revealed that 13,519 ha (more than 63% of the total agricultural area) remained fallow during the dry season. The majority of these are concentrated in the hilly regions of the district. These single crop areas can be cultivated by introducing water-efficient crops such as vegetables, lentils, and pulses, or could invest further in the irrigation to facilitate the perennial irrigation facility. Given the availability of irrigation facilities, a large proportion of areas will convert to suitable areas for the cultivation of high-value winter crops such as potato, tomato, cauliflower, and other vegetables, medicinal plants, or even fruits such as apples at higher altitude and oranges or kiwis in lower altitude. Thus, the obtained crop intensity maps and statistics offer further investment to intensify crop patterns and improve the livelihood of local farmers.

This study focused on using Sentinel 2 optical imagery to keep track of seasonal crop dynamics. However, Sentinel 1 microwave dataset would be instrumental with the coupling of optical imageries to detect cropping patterns and could yield a better result in the monsoon seasons, as microwave remote sensing is all-weather remote sensing and has little or no effect due to the cloud cover. Cloud contamination is one of the biggest challenges in using optical remote sensing images in high mountainous regions. As we obtained promising results through the semi-automatic processing of the freely available Sentinel 2 A/B dataset for the Kaski district, the method is applicable to keep track of seasonal crop dynamics across the country, region, or global scale.

## 5. Conclusions

We developed a semi-automatic rule-based workflow that effectively captures seasonal dynamics and maps cropping intensity using time-series NDVI data from Sentinel 2A and 2B satellites, coupled with farmer knowledge. This workflow has been applied to the complex topography of the Himalayas of Nepal, utilizing unsupervised ISODATA clustering to extract agricultural areas, and a phenology-based method using GDEM elevation and slope data to automatically map seasonal cropping patterns and intensity. This was coupled with farmer knowledge regarding the common crops in the region and their calendar, to obtain the seasonal crop information.

The resultant maps had an overall accuracy of 82%, with a Kappa coefficient of 0.74 for the Kaski district. We were able to detect a maximum of three cropping cycles: the first

starting in March–May and ending in June–August, the second starting in November–December and ending in March–May, and the third starting between June and August and ending in February–May. The accuracy of cropping intensity was excellent, with 88% accuracy and a 0.83 Kappa coefficient at a 10 m spatial resolution.

We found that a significant proportion of arable land was single cropped, leaving these areas fallow during other seasons. However, we believe that intensifying crop production in these areas could provide an opportunity to increase agricultural production and combat potential food insecurity in the future.

In conclusion, this study provides valuable insights into innovative agricultural planning at the district level and highlights the potential for similar work to be extended across the country and various regions. As such, it remains an essential case for policymakers and planners to consider as they work towards improving agriculture and food security in Nepal.

**Supplementary Materials:** The developed system has been made public and all the relevant sources along with the user manual are available at the following link: [https://github.com/bgmishra/Crop\\_monitoring](https://github.com/bgmishra/Crop_monitoring) (accessed on 2 April 2023).

**Author Contributions:** Conceptualization, B.M.; methodology, B.M.; software, B.M., A.D., R.B. and D.M.B.; validation, A.D., R.B. and N.L.; formal analysis, R.B., D.M.B. and N.L.; investigation R.B. and D.M.B.; resources, B.M. and K.P.B.; data curation, B.M., R.B., D.M.B. and N.L.; writing—original draft preparation, B.M., K.P.B., S.P. and S.P.; writing—review and editing, B.M. and S.P.; visualization, B.M., D.M.B., R.B. and N.L.; project administration, K.P.B.; funding acquisition, K.P.B. and B.M. All authors have read and agreed to the published version of the manuscript.

**Funding:** This research was partially funded by Ministry of Land Management, Agriculture and Cooperative, Gandaki Province Pokhara, Nepal.

**Informed Consent Statement:** Not applicable.

**Data Availability Statement:** Google Earth Engine.

**Conflicts of Interest:** The authors declare no conflict of interest.

## References

1. Kubo, M.; Purevdorj, M. The Future of Rice Production and Consumption. *J. Food Distrib. Res.* **2004**, *35*, 128–142.
2. Parry, M.L.; Rosenzweig, C.; Iglesias, A.; Livermore, M.; Fischer, G. Effects of Climate Change on Global Food Production under SRES Emissions and Socio-Economic Scenarios. *Glob. Environ. Chang.* **2004**, *14*, 53–67. [[CrossRef](#)]
3. Laborte, A.G.; Paguirigan, N.C.; Moya, P.F.; Nelson, A.; Sparks, A.H.; Gregorio, G.B. Farmers' Preference for Rice Traits: Insights from Farm Surveys in Central Luzon, Philippines, 1966–2012. *PLoS ONE* **2015**, *10*, e0136562. [[CrossRef](#)]
4. Fritz, S.; See, L.; Bayas, J.C.L.; Waldner, F.; Jacques, D.; Becker-Reshef, I.; Whitcraft, A.; Baruth, B.; Bonifacio, R.; Crutchfield, J.; et al. A Comparison of Global Agricultural Monitoring Systems and Current Gaps. *Agric. Syst.* **2019**, *168*, 258–272. [[CrossRef](#)]
5. Kang, Y.; Khan, S.; Ma, X. Climate Change Impacts on Crop Yield, Crop Water Productivity and Food Security—A Review. *Prog. Nat. Sci.* **2009**, *19*, 1665–1674. [[CrossRef](#)]
6. Whitcraft, A.K.; Becker-Reshef, I.; Justice, C.O. Agricultural Growing Season Calendars Derived from MODIS Surface Reflectance. *Int. J. Digit. Earth* **2015**, *8*, 173–197. [[CrossRef](#)]
7. Ye, X.I.N.; Yang, X.-Y.; Zhou, B.-R.; Wang, D.-J.; Zhou, H.-K.; Xu, W.-X.; Yao, B.-Q.; Ma, Z.; Li, Y.-K.; Yang, Y.-S.; et al. Relationship Between Phenology, Productivity, And Meteorological Factors in Recent 15 Years in the Pastoral Area of Qinghai, China. *Int. J. Big Data Min. Glob. Warm.* **2019**, *1*, 1950002. [[CrossRef](#)]
8. Schenk, P.M.; McGrath, K.C.; Lorito, M.; Pieterse, C.M.J. Plant–Microbe and Plant–Insect Interactions Meet Common Grounds. *New Phytol.* **2008**, *179*, 251–256. [[CrossRef](#)]
9. Giron, D.; Dubreuil, G.; Bennett, A.; Dedeine, F.; Dicke, M.; Dyer, L.A.; Erb, M.; Harris, M.O.; Huguet, E.; Kaloshian, I.; et al. Promises and Challenges in Insect–Plant Interactions. *Entomol. Exp. Appl.* **2018**, *166*, 319–343. [[CrossRef](#)]
10. Li, H.; Zhu, H.; Qiu, L.; Wei, X.; Liu, B.; Shao, M. Response of Soil OC, N and P to Land-Use Change and Erosion in the Black Soil Region of the Northeast China. *Agric. Ecosyst. Environ.* **2020**, *302*, 107081. [[CrossRef](#)]
11. Sun, T.; Feng, X.; Lal, R.; Cao, T.; Guo, J.; Deng, A.; Zheng, C.; Zhang, J.; Song, Z.; Zhang, W. Crop Diversification Practice Faces a Tradeoff between Increasing Productivity and Reducing Carbon Footprints. *Agric. Ecosyst. Environ.* **2021**, *321*, 107614. [[CrossRef](#)]
12. Duflot, R.; San-Cristobal, M.; Andrieu, E.; Choisis, J.-P.; Esquerré, D.; Ladet, S.; Ouin, A.; Rivers-Moore, J.; Sheeren, D.; Sirami, C.; et al. Farming Intensity Indirectly Reduces Crop Yield through Negative Effects on Agrobiodiversity and Key Ecological Functions. *Agric. Ecosyst. Environ.* **2022**, *326*, 107810. [[CrossRef](#)]

13. Johansson, J.; Nilsson, J.Å.; Jonzén, N. Phenological Change and Ecological Interactions: An Introduction. *Oikos* **2015**, *124*, 1–3. [[CrossRef](#)]
14. Shammi, S.A.; Meng, Q. Use Time Series NDVI and EVI to Develop Dynamic Crop Growth Metrics for Yield Modeling. *Ecol. Indic.* **2021**, *121*, 107124. [[CrossRef](#)]
15. Groten, S.M. NDVI-Crop Monitoring and Early Yield Assessment of Burkina Faso. *Int. J. Remote Sens.* **1993**, *14*, 1495–1515. [[CrossRef](#)]
16. Seo, B.; Lee, J.; Do Lee, K.; Hong, S.; Kang, S. Improving Remotely-Sensed Crop Monitoring by NDVI-Based Crop Phenology Estimators for Corn and Soybeans in Iowa and Illinois, USA. *F. Crop. Res.* **2019**, *238*, 113–128. [[CrossRef](#)]
17. Li, C.; Li, H.; Li, J.; Lei, Y.; Li, C.; Manevski, K.; Shen, Y. Using NDVI Percentiles to Monitor Real-Time Crop Growth. *Comput. Electron. Agric.* **2018**, *162*, 357–363. [[CrossRef](#)]
18. Boschetti, M.; Busetto, L.; Manfron, G.; Laborte, A.; Asilo, S.; Pazhanivelan, S.; Nelson, A. PhenoRice: A Method for Automatic Extraction of Spatio-Temporal Information on Rice Crops Using Satellite Data Time Series. *Remote Sens. Environ.* **2017**, *194*, 347–365. [[CrossRef](#)]
19. Sakamoto, T.; Yokozawa, M.; Toritani, H.; Shibayama, M.; Ishitsuka, N.; Ohno, H. A Crop Phenology Detection Method Using Time-Series MODIS Data. *Remote Sens. Environ.* **2005**, *96*, 366–374. [[CrossRef](#)]
20. More, R.S.; Manjunath, K.R.; Jain, N.K.; Panigrahy, S.; Parihar, J.S. Derivation of Rice Crop Calendar and Evaluation of Crop Phenometrics and Latitudinal Relationship for Major South and South-East Asian Countries: A Remote Sensing Approach. *Comput. Electron. Agric.* **2016**, *127*, 336–350. [[CrossRef](#)]
21. Bandaru, V.; Yaramasu, R.; PNVR, K.; He, J.; Fernando, S.; Sahajpal, R.; Wardlow, B.D.; Suyker, A.; Justice, C. PhenoCrop: An Integrated Satellite-Based Framework to Estimate Physiological Growth Stages of Corn and Soybeans. *Int. J. Appl. Earth Obs. Geoinf.* **2020**, *92*, 102188. [[CrossRef](#)]
22. Mishra, B.; Busetto, L.; Boschetti, M.; Laborte, A.; Nelson, A. RICA: A Rice Crop Calendar for Asia Based on MODIS Multi Year Data. *Int. J. Appl. Earth Obs. Geoinf.* **2021**, *103*, 102471. [[CrossRef](#)]
23. Kumar, A.; Roy, D.; Joshi, P.K.; Tripathi, G.; Adhikari, R.P. Impact of Contract Farming on Profits and Yield of Smallholder Farms in Nepal: An Evidence from Lentil Cultivation. *Agric. Appl. Econ. Assoc. Annu. Meet.* **2016**, *33*. [[CrossRef](#)]
24. Rimal, B.; Zhang, L.; Rijal, S. Crop Cycles and Crop Land Classification in Nepal Using MODIS NDVI. *Remote Sens. Earth Syst. Sci.* **2018**, *1*, 14–28. [[CrossRef](#)]
25. Karki, R.; Talchabhadel, R.; Aalto, J.; Baidya, S.K. New Climatic Classification of Nepal. *Theor. Appl. Climatol.* **2016**, *125*, 799–808. [[CrossRef](#)]
26. Mishra, B.; Babel, M.S.; Tripathi, N.K. Analysis of Climatic Variability and Snow Cover in the Kaligandaki River Basin, Himalaya, Nepal. *Theor. Appl. Clim.* **2014**, *116*, 681–694. [[CrossRef](#)]
27. MOALD. *Statistical Information in Nepalese Agriculture 2075/76*; Singha Durbar: Kathmandu, Nepal, 2020.
28. Carman, C.S.; Merickel, M.B. Supervising ISODATA with an Information Theoretic Stopping Rule. *Pattern Recognit.* **1990**, *23*, 185–197. [[CrossRef](#)]
29. Cleveland, W.S. Robust Locally Weighted Regression and Smoothing Scatterplots. *J. Am. Stat. Assoc.* **1979**, *74*, 829–836. [[CrossRef](#)]
30. Jacoby, W.G. Loess: A Nonparametric, Graphical Tool for Depicting Relationships between Variables. *Elect. Stud.* **2000**, *19*, 577–613. [[CrossRef](#)]
31. Fox, J.; Weisberg, S. *Nonparametric Regression*; SAGE: Newcastle, UK, 2016.
32. Patel, J.H.; Oza, M.P. Deriving Crop Calendar Using NDVI Time-Series. *Int. Arch. Photogramm. Remote Sens. Spat. Inf. Sci. ISPRS Arch.* **2014**, *XL-8*, 869–873. [[CrossRef](#)]
33. Bastola, A.; Karki, T.; Marahatta, S.; Amgain, L.P. Growth, Phenology, Yield and Yield Attributes of Rice as Influenced by Tillage, Residue and Nitrogen Management Practice in Chitwan, Nepal. *Afr. J. Agric. Res.* **2021**, *17*, 128–136.
34. Dahal, S.; Karki, T.B.; Amgain, L.P.; Bhattachan, B.K. Tillage, Residue, Fertilizer and Weed Management on Phenology and Yield of Spring Maize in Terai, Nepal. *Int. J. Appl. Sci. Biotechnol.* **2014**, *2*, 328–335. [[CrossRef](#)]
35. Aman, K.C.; Acharya, T.D.; Wagle, N.; Lee, D.H. Tracking Long-Term Phenological Shift in Response to Climatic Parameters in Chitwan National Park, Nepal. *Sensors Mater.* **2021**, *33*, 3787–3799.
36. Luintel, N.; Ma, W.; Ma, Y.; Wang, B.; Xu, J.; Dawadi, B.; Mishra, B. Tracking the Dynamics of Paddy Rice Cultivation Practice through MODIS Time Series and PhenoRice Algorithm. *Agric. For. Meteorol.* **2021**, *307*, 108538. [[CrossRef](#)]
37. Sisheber, B.; Marshall, M.; Ayalew, D.; Nelson, A. Tracking Crop Phenology in a Highly Dynamic Landscape with Knowledge-Based Landsat–MODIS Data Fusion. *Int. J. Appl. Earth Obs. Geoinf.* **2022**, *106*, 102670. [[CrossRef](#)]
38. Kontgis, C.; Schneider, A.; Ozdogan, M. Mapping Rice Paddy Extent and Intensi Fi Cation in the Vietnamese Mekong River Delta with Dense Time Stacks of Landsat Data. *Remote Sens. Environ.* **2015**, *169*, 255–269. [[CrossRef](#)]
39. Jain, M.; Mondal, P.; DeFries, R.S.; Small, C.; Galford, G.L. Mapping Cropping Intensity of Smallholder Farms: A Comparison of Methods Using Multiple Sensors. *Remote Sens. Environ.* **2013**, *134*, 210–223. [[CrossRef](#)]

**Disclaimer/Publisher’s Note:** The statements, opinions and data contained in all publications are solely those of the individual author(s) and contributor(s) and not of MDPI and/or the editor(s). MDPI and/or the editor(s) disclaim responsibility for any injury to people or property resulting from any ideas, methods, instructions or products referred to in the content.